JACS
JOURNAL OF THE AMERICAN CHEMICAL SOCIETY
Article
Cite This: J. Am. Chem. Soc. XXXX, XXX, XXX−XXX
pubs.acs.org/JACS

Time-Dependent Switching of Constitutional Dynamic Libraries and Networks from Kinetic to Thermodynamic Distributions

Meixia He and Jean-Marie Lehn*

Laboratoire de Chimie Supramoléculaire, Institut de Science et d'Ingénierie Supramoléculaires (ISIS), Université de Strasbourg, 8 Allée Gaspard Monge, 67000 Strasbourg, France

Supporting Information

ABSTRACT: The distribution of the constituents of a constitutional dynamic library (CDL) may undergo time-dependent changes as a function of the kinetics of the processes generating the CDL from its components. Thus, the constitutional dynamic network (CDN) representing the connections between the constituents changes from a kinetic distribution to the thermodynamic one as a function of time. We investigated the behavior of dynamic covalent libraries (DCLs) of four constituents generated by reversible formation of C═N bonds between four components, 2 aldehydes and 2 amino compounds, both in absence and in the presence of metal cations. The associated [2 × 2] networks underwent time-dependent changes from the initial kinetic distribution to the final thermodynamic one, involving an orthogonal switch from one diagonal to the other diagonal of the square [2 × 2] network leading to a very large change in distribution. The DCL constituents could be switched from kinetic products (imines) to thermodynamic products (oximes or acylhydrazones) based on the reactivities of the components and the thermodynamic stabilities of the constituents without addition of any external effector, solely on the basis of the intrinsic properties of the self-contained system. Such processes were achieved for purely organic DCLs/CDNs as well as for inorganic ones containing two metal cations, the latter changing from the silver(I) complex of an imine (kinetic product) to the zinc(II) complex of a hydrazone (thermodynamic product). The results bear relationship to out-of-equilibrium systems concerning kinetic behavior in adaptive chemistry.

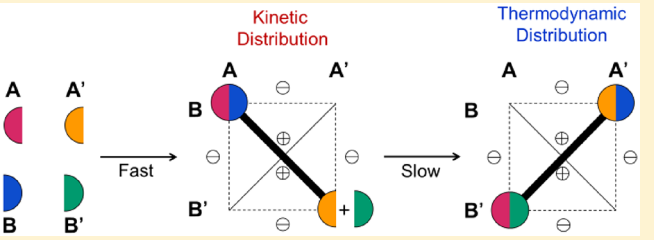

1. INTRODUCTION

The design, construction, and study of networks of interconnected entities bear great significance for the understanding and control of the behavior of complex systems[1] in chemistry and biology involving for instance the regulation of interdependent reactions. A special case of particular interest is that of dynamic networks connecting chemical entities of different constitutions on molecular and supramolecular levels as presented in constitutional dynamic chemistry (CDC).[1c,2] Such constitutional dynamic networks (CDNs)[3] link the sets of chemical entities forming constitutional dynamic libraries (CDLs),[4] that undergo constitutional variation either by internal rearrangement or by exchange, incorporation, and extrusion of components through reversible formation of covalent and noncovalent linkages. As a consequence of this dynamicity, the dynamic system may be shifted from one constitutional state to another one in response to physical stimuli (such as light,[5] temperature,[3d,5g,6] pressure,[7] and various other factors[3e,8]) or chemical effectors (metal cations,[9] protons,[3d,10] reactive molecules,[11] and self-sorting[12]), thus achieving adaptation. A particular case is that where the system adapts to a shape switching resulting from a change of the molecular geometry of a component.[13] The variations in the distribution of the members of a CDL are determined by the nature of the relationship between constituents which may be of either agonistic or antagonistic nature and lead to either simultaneous amplification/up-regulation or down-regulation of the responsive constituent(s), respectively.[9c]

On the molecular level, the reversible formation of C═N bonds from a carbonyl group and an amino group to give imine-type compounds (imines,[14] hydrazones,[15] acylhydrazones,[16] and oximes[15a,17]) has been extensively used to set up dynamic covalent libraries (DCLs) of various types. It presents a wide range of rates[18] and thermodynamic features[19] and is a reaction of fundamental importance.[2e] Relative rates of C═N formation will lead to time-dependent changes in the composition of a DCL representing the kinetic evolution of the system.[3f,20] From previous studies, imines are known to form rapidly, whereas oximes and acylhydrazones are formed more slowly but have higher thermodynamic stabilities at equilibrium.[20] Relevant cases in line with these results are found in the experiments shown below.

Unlike the variations induced by an external agent,[5−12] the internal features of a DCL may lead to a time-dependent change in the distribution of the constituents according to its kinetic and thermodynamic properties.[3f,20]

Received: August 30, 2019

DOI: 10.1021/jacs.9b09395
J. Am. Chem. Soc. XXXX, XXX, XXX−XXX

A particularly interesting case is that where the DCL undergoes *network switching* from an initial kinetic distribution of constituents determined by reaction rates, to the final thermodynamic distribution at equilibrium, in a sort of kinetic adaptation or *adaptation to time*.

The above considerations prompted us to design systems based on multiple components possessing different structural and electronic properties to selectively adjust the kinetic and thermodynamic products within the DCL. We thus designed libraries of four constituents generated from two aldehydes **A**, **A′** and two amino compounds **B**, **B′** and investigated their kinetic and thermodynamic properties which lead to component selection and amplification of the different constituents as a function of time (Scheme 1). Such a DCL is represented by a

Scheme 1. Evolution of a DCL of Four Constituents Undergoing a Time-Dependent Orthogonal Switching of Its Associated [2 × 2] CDN from One Diagonal to the Other One

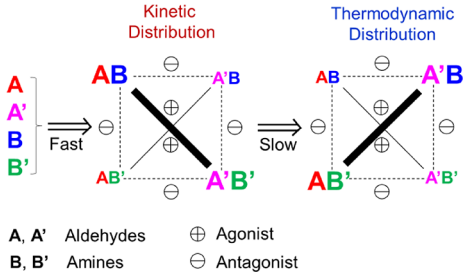

square [2 × 2] CDN with the four constituents **AB**, **AB′**, **A′B**, and **A′B′** at the corners, linking antagonistic constituents (e.g., **AB** and **A′B**) along the edges and agonistic ones (**AB** and **A′B′**; **AB′** and **A′B**) through the diagonals as presented earlier.[3d] The antagonists (e.g., **AB** and **AB′**) share one common component so that when the amount of one of them increases, that of the other one will decrease. In contrast, the agonists (e.g., **AB** and **A′B′**) share no component, so that an increase in the amount of one constituent will enforce the enhancement of the other one, in an *agonist amplification* manner. When all of the constituents have similar energy, a near-statistical distribution is obtained.[9d] By selecting aldehydes and amino compounds with appropriate properties, the library may be made to contain initially almost exclusively one pair of diagonally located constituents as kinetic products **AB** and **A′**+**B′** (here initially unreacted but amplified agonistic components) and evolve with time (as observed by ^{1}H NMR spectroscopy[21] toward the orthogonal pair of constituents as thermodynamic products **AB′** and its agonist **A′B**, thus achieving *kinetic network switching* of the system (Scheme 1) as observed.[22]

2. RESULTS AND DISCUSSION

2.1. Kinetic Switching of a Constitutional Dynamic Network——Kinetic vs Thermodynamic Distributions in Dynamic Covalent Libraries of Imino Compounds. *2.1.1. Component Selection in Competitive Reactions.* With the goal of designing four-component systems suitable for achieving kinetic switching of constitutional dynamic networks, *three-component experiments* were first performed to determine their kinetic behaviors in a competitive setup. Two constituents were generated by the reaction of pyridine-2-carboxaldehyde or benzaldehyde derivatives with amines and hydroxylamines or hydrazides. The pyridine aldehyde is known to be more reactive than benzaldehyde and can also generate an NN bidentate or NNO tridentate coordination site for metal cation binding by reaction with amines or hydrazides.[23] As mentioned above, amines, together with hydroxylamines or hydrazides, were chosen because of the differences in the thermodynamic stabilities of their imino products.[19,20]

First, we investigated competitive imine and oxime formation from the three components **A1**, **B1**, **B2**, to check their relative rates. Equal amounts of each component were mixed in CD_3CN at room temperature. After less than 5 min, only the imine **A1B1** was detected as the kinetic product and no oxime was observed at this moment. After 24 h, the imine was largely converted into the oxime **A1B2** as the thermodynamic product (see Table S1 in the Supporting Information, SI). The evolution of the ^{1}H NMR spectra is presented in Figure 1a. The corresponding kinetic traces (Figure 1b) show the crossing of formation curves of **A1B1** and **A1B2**. Similar experiments were conducted for the set [**A2** + **B1** + **B2**] containing the much less reactive aldehyde **A2** to further explore the design and the kinetics of such DCLs. The reactions were now much slower and allowed for a better observation of the beginning of the process (Figure 1c, d and Table S2). The corresponding separate experiments of imine **A1B1**, **A2B1** and oxime **A1B2**, **A2B2** formation are shown in the SI (Figures S26−S33, Tables S3−S7).

The reaction in the set of [**A1** + **A2** + **B1**] was also studied, but the exchange reaction was too slow to follow due to the low reactivity of **A2** (see Figures S34 and S35 of the SI). The set [**A1** + **A2** + **B2**] may be expected to behave similarly. The results above (Figure 1) confirm that, as expected, in both cases, the imine is the kinetic product while the oxime is the thermodynamic one.

2.1.2. Kinetic and Thermodynamic Features of Three DCLs ([1], [2], and [3]) of Four Constituents Generated from Four Components. 2.1.2.1. DCL[1]. After mixing the four components **A1**, **A2**, **B1**, **B2** in CD_3CN (30 mM each), the composition of the **DCL**[**1**] was monitored by ^{1}H NMR spectroscopy[21,22] as a function of time. As seen in the ^{1}H NMR spectra shown in Figure 2, **A1B1** was detected as the main component within 25 min together with **A1B2**, **A2B1**, and **A2B2** formed in a biased distribution of 36%, 13%, 6%, and 1%, respectively, as well as 44% free **A2** and 37% free **B2** and 10% free **B1** (Scheme 2). **A1B1** was the overwhelming kinetic product of the DCL. As such, it should amplify its agonist constituent **A2B2**, which was however not detected at this stage, due to the low reactivities of **A2** and **B2**, which stayed in the free form. The reason for this biased kinetic distribution may be attributed to the comparatively fast formation of imine **A1B1** with respect to that of the oxime **A1B2**. As seen above, the competitive reactions performed for (i) **A1** with **B1** and **B2** (Figure 1a) (ii) **A2** with **B1** and **B2** (Figure 1c) as well as (iii) **B1** with **A1** and **A2** (Figures S34 and S35) showed that **A1** and **B1** are as expected more reactive than **A2** and **B2**, respectively. Over time, the oxime **A1B2** progressively formed together with its agonist **A2B1**, generated concomitantly from the initially unreacted **A2** and **B2**, whereas at the same time the imine **A1B1** decreased. After about 15 h, the initial components had almost fully reacted and only the four expected constituents were present. The composition of the DCL was finally 14.0%/36%/35%/13% for the constituents **A1B1**, **A1B2**, **A2B1**, **A2B2**, respectively (Scheme 2, Table S8). The process thus realizes a kinetic switching of the CDN associated with **DCL**[**1**] from the diagonal [**A1B1**, **A2** + **B2**] to the orthogonal agonists diagonal [**A1B2**, **A2B1**]. The kinetic traces show the corresponding

DOI: 10.1021/jacs.9b09395
J. Am. Chem. Soc. XXXX, XXX, XXX−XXX

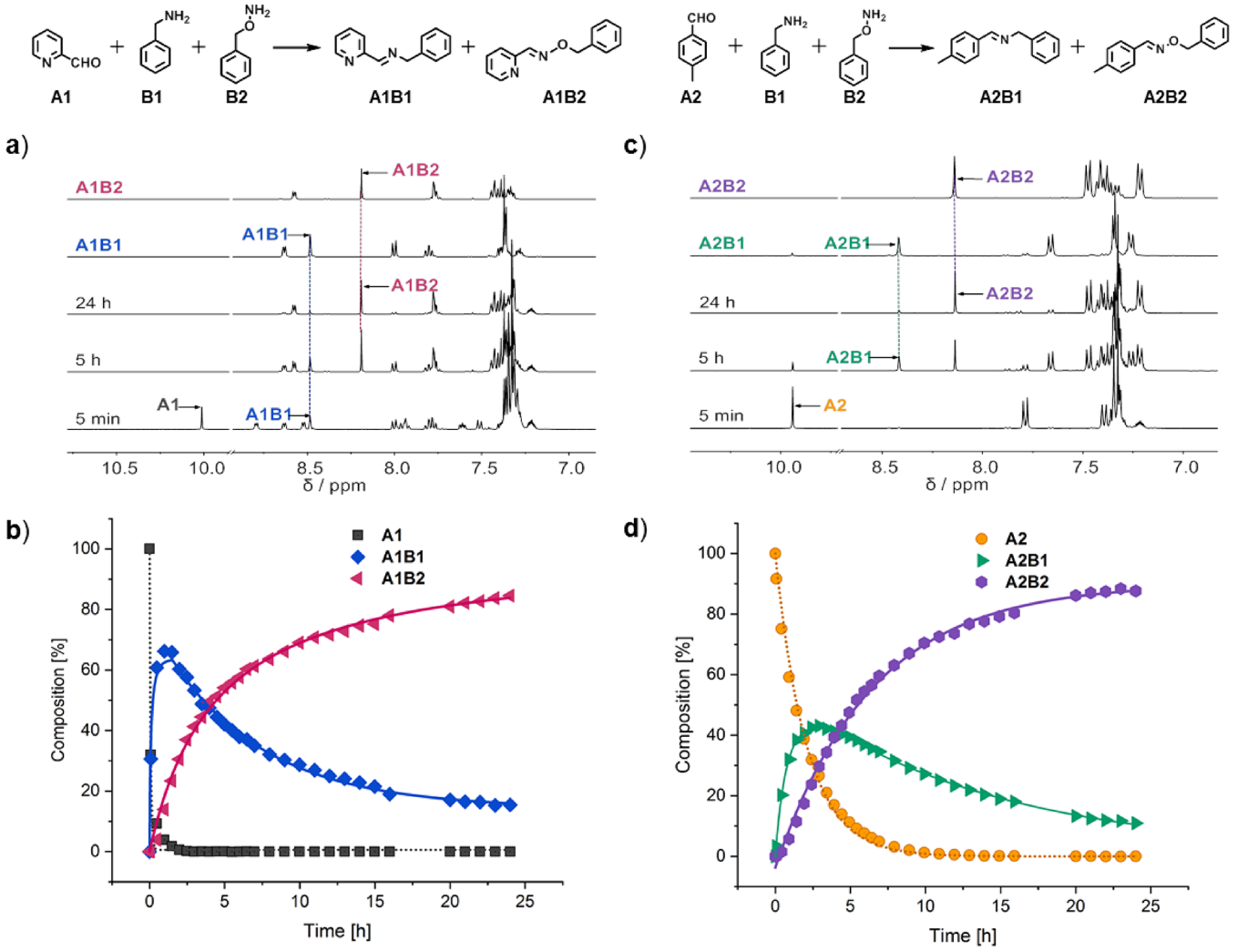

Figure 1. (Top) Evolution of the ^{1}H NMR (400 MHz) spectra of the mixtures generated from equal amounts of components (a) **A1** + **B1** + **B2** (three bottom traces) and (c) **A2** + **B1** + **B2** (three bottom traces) after respectively 5 min, 5 h, and 24 h (from the bottom). The two top traces are the spectra of the isolated constituents **A1B1** and **A1B2** (left), **A2B1** and **A2B2** (right), respectively. The arrows indicate the aldehyde CHO proton (9.5−10.0 ppm region) and imine CH═N proton NMR signals of the compounds. (Bottom) Kinetic plots of the evolution as a function of time of the compounds in the mixtures generated from equal amounts of components (b) **A1** + **B1** + **B2** and (d) **A2** + **B1** + **B2**, corresponding to the NMR spectra above. The composition % data have been obtained by integration of the imine CH═N and aldehyde CHO proton signals in ^{1}H NMR spectra (30 mM each, CD_3CN, r.t.). For clarity, the kinetic curves are shown for only some of the compounds (see also notes S21 and S22, Tables S1 and S2).

evolution with line crossings (Figure 3). Similar results were obtained when **A2** was replaced by *p*-chlorobenzaldehyde **A4** or by *p*-fluorobenzaldehyde **A5**, which however were more reactive (as shown in Schemes S1 and S2, Figures S36−S39, and Tables S9 and S10).

2.1.2.2. DCL[2]. In order to explore the requirements for obtaining a kinetic network switching, an experiment similar to that in **DCL**[**1**] was performed with **DCL**[**2**] formed by components **A3**, **A4**, **B1**, and **B2** (Scheme S3). From the ^{1}H NMR spectra (Figure S40), the behavior of this **DCL**[**2**] was similar to that of **DCL**[**1**] described above. After 4 min, four components **A3B1**, **A3B2**, **A4B1**, and **A4B2** were obtained, giving a biased distribution of 32%, 14%, 6%, < 1% (Scheme S3, Figure S41, and Table S11) with the percentage of free **A4** and **B2** being 44% and 36%. The reason for this bias may again be attributed to the fast formation of imine **A3B1** rather than that of the oxime **A3B2** due to the low reactivity of **A4** compared to **A3** as well as of **B2** compared to **B1** (shown Figures S42−S47, Tables S12−S13) as confirmed by the separate competitive reactions. As shown in the evolution of the ^{1}H NMR spectra and the kinetic traces (Figures S40 and S41), this initial **DCL**[**2**] underwent reorganization with time and shifted to a composition where the oxime **A3B2** was the thermodynamic product, resulting also in the amplification of its diagonal agonist **A4B1**. The composition of the library became then 9%, 41%, 43%, and 7% for the constituents **A3B1**, **A3B2**, **A4B1**, and **A4B2**, respectively. Like in case **DCL**[**1**] above, the process realizes again a kinetic switching of the CDN associated with **DCL**[**2**] from the diagonal [**A3B1**, **A4** + **B2**] to the orthogonal agonist diagonal [**A3B2**, **A4B1**].

2.1.2.3. DCL[3]. Finally a third four component **DCL**[**3**] was studied in the same conditions as for **DCL**[**1**] and **DCL**[**2**] above, based on the components **A3**, **A4**, **B1**, and the *N*-methylbenzohydrazide **B3** (Scheme 3). The formation of the four constituents **A3B1**, **A3B3**, **A4B1**, and **A4B3** was again monitored by ^{1}H NMR as a function of time. Similarly to oximes, acylhydrazones are known to be thermodynamically favored products relative to simple imines.[20] **B3** was selected to

DOI: 10.1021/jacs.9b09395
J. Am. Chem. Soc. XXXX, XXX, XXX−XXX

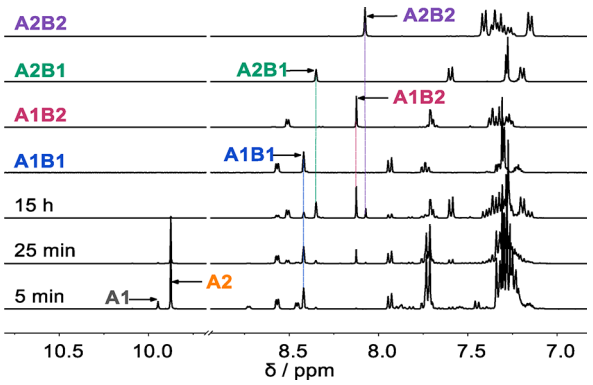

Figure 2. Evolution of ^{1}H NMR (400 MHz) spectra of the compounds generated from the **DCL**[**1**] mixture of equal amounts of **A1**, **A2**, **B1**, **B2** (30 mM each in CD_3CN, r.t.) after 5 min, 25 min and 15 h (three bottom traces). The four top traces correspond to the isolated constituents **A1B1**, **A1B2**, **A2B1**, and **A2B2**. The arrows indicate the aldehyde CHO proton (9.5−10.0 ppm region) and imine CH═N proton NMR signals of the compounds.

Scheme 2. Kinetic Switching of the [2 × 2] CDN Formed by the DCL[1] Set of Components [A1 + A2 + B1 + B2] (top) from the [A1B1, A2 + B2] State (Middle Left) to the Orthogonal State [A1B2, A2B1] (Middle Right) in CD_3CN at Room Temperature[a]

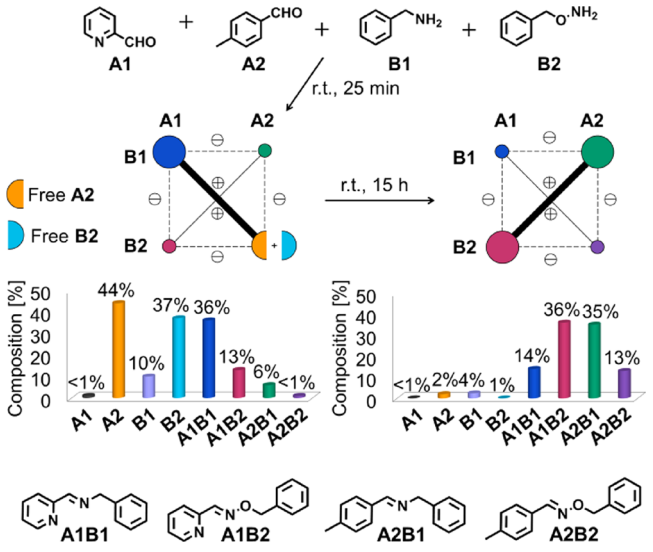

[a]The indicated composition % values of the different compounds present correspond to reaction times of 25 min (left) and 15 h (right), see also Table S8 in SI. Data obtained from the 400 MHz ^{1}H NMR spectra (see Figures 2 and 3).

replace **B2** to investigate how this new DCL would behave. After 5 min, only two products were detected, giving a composition **A3B1** 48%, **A4B1** 6%, together with 43% of **A4** and 50% of **B3** left unreacted in the solution. After 96 h at room temperature, the reaction reached an equilibrium with a constituent composition of **A3B1** 9%, **A3B3** 41%, **A4B1** 38%, and **A4B3** 12%. As shown in the evolution of the ^{1}H NMR spectra and the kinetic traces (Figures 4, 5, and Table S14), the **DCL**[**3**] showed again an evolution from an initial kinetic distribution to the final thermodynamic distribution with an orthogonal switching of the associated CDN from the diagonal axis [**A3B1**, **A4** + **B3**] to the orthogonal [**A3B3**, **A4B1**] one. Interestingly, the initial distribution showed <1% of the acylhydrazone **A3B3** compared

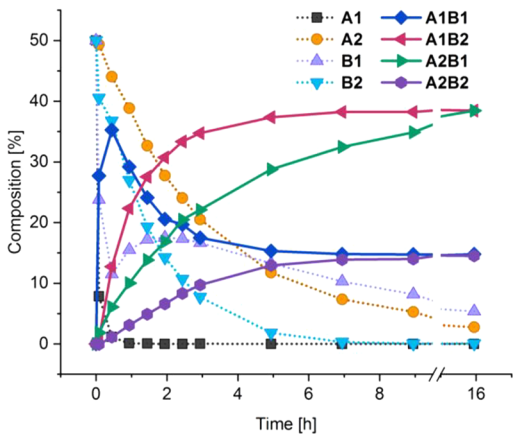

Figure 3. Kinetic plots of the evolution of the compounds generated from a mixture of equal amounts of components **A1** + **A2** + **B1** + **B2** as a function of time over 16 h. The composition % data have been obtained by integration of the imine CH═N and aldehyde CHO proton signals in the 400 MHz ^{1}H NMR spectra (30 mM each, CD_3CN, r.t.). The lines are not calculated but just introduced to guide the eye (see also notes S21 and S22).

Scheme 3. Kinetic Switching of the [2 × 2] CDN Formed by the DCL[3] Set of Components [A3 + A4 + B1 + B3] (top) from the [A3B1, A4 + B3] State (Middle Left) To the Orthogonal State [A3B3, A4B1] (Middle Right) in CD_3CN at Room Temperature[a]

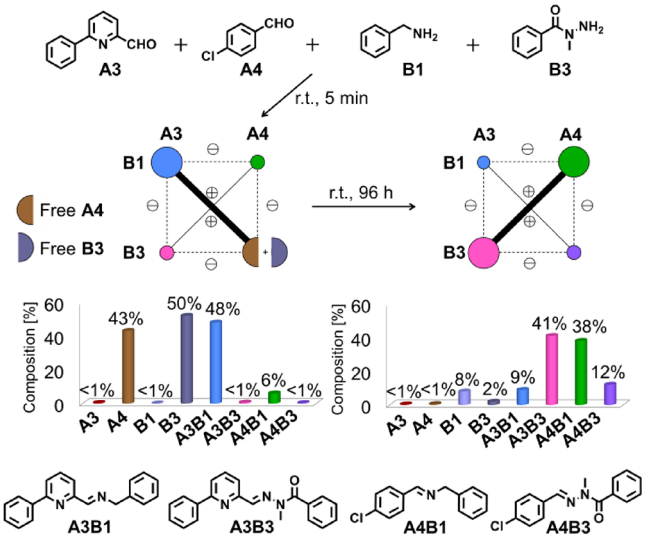

[a]The indicated composition % values of the different compounds present correspond to reaction times of 5 min (left) and 96 h (right), see also **Table S14** in SI. Data obtained from the 400 MHz ^{1}H NMR spectra (see Figures 4 and 5).

to 14% for the corresponding oxime **A3B2** in the **DCL**[**2**] above, indicating an appreciably lower reactivity of the (*N*-methylated) hydrazide **B3** compared to the alkoxy amine **B2**. This feature is also reflected in the fact that the evolution of the kinetic traces (Figure 5) are more gradual than in the previous cases above. Indeed, a separate competition experiment between **B2** and **B3** reacting with **A3** in 1:1:1 ratio yielded 21% of **A3B2** and 3% of **A3B3** after 8 days showing that **A3B2** is thermodynamically preferred over **A3B3** (Figures S48, S49, and Table S15). On the kinetic level, the same reaction in 1:1:2 stoichiometry (Figures S50, S51, and Table S16) gave after 7 days 17% of **A3B2** and 4%

DOI: 10.1021/jacs.9b09395
J. Am. Chem. Soc. XXXX, XXX, XXX−XXX

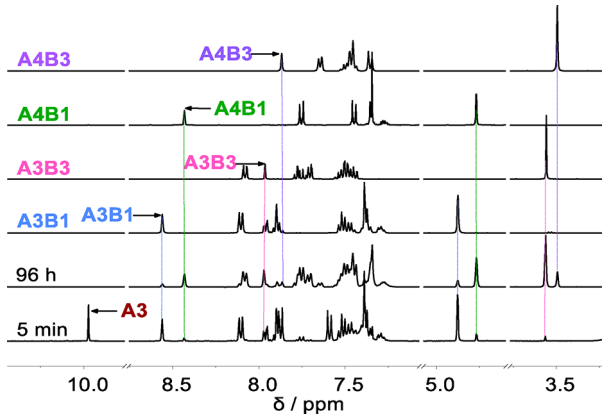

Figure 4. Evolution of ^{1}H NMR (400 MHz) spectra of the compounds generated from the **DCL**[**3**] mixture of equal amounts of **A3**, **A4**, **B1**, and **B3** (30 mM each in CD_3CN, r.t.) after 5 min and 96 h (two bottom traces). The four top traces correspond to the isolated constituents **A3B1**, **A3B3**, **A4B1**, and **A4B3**. The arrows indicate the aldehyde CHO proton (9.5−10.0 ppm region) and imine CH═N proton NMR signals of the compounds.

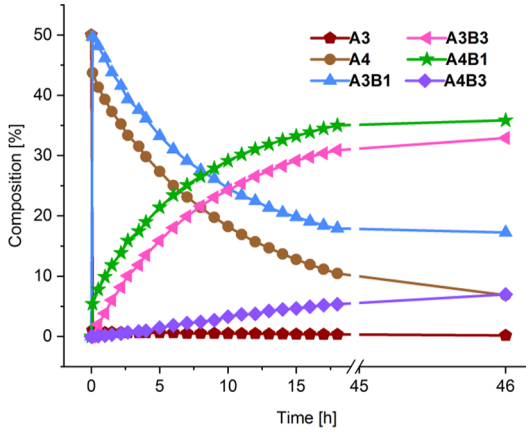

Figure 5. Kinetic plots of the evolution of a mixture of equal amounts of components **A3** + **A4** + **B1** + **B3** as a function of time. The composition % data have been obtained by integration of the imine $-CH_2-$ (of the benzyl group), hydrazone $N-CH_3$ and aldehyde CHO proton signals in the 400 MHz ^{1}H NMR spectra (30 mM each, CD_3CN, r.t.). For clarity, the kinetic curves are shown for only some of the compounds (see also notes S21 and S22).

of **A3B3** with large amount of unreacted **A3**, indicating also that the alkoxy amine **B2** reacted faster than the hydrazide **B3**. In the case of the set of components **A1** + **A3** + **B1** + **B3** (Scheme S4), the similar reactivities of **A1** and **A3** (6-phenyl derivative of **A1**) led to two imines **A3B1** (40%) and **A1B1** (29%) as kinetic products (5 min) with some **A3** (10%) and **A1** (20%) unreacted in the solution. At equilibrium they finally reached a near-statistical distribution for **A3B1** (19%), **A1B1** (25%), **A3B3** (32%), and **A1B3** (21%) (see data in Figures S52, S53, and Table S17).

The present DCLs all undergo a network switching from a kinetic distribution to the thermodynamic distribution as a function of time. This process that may be considered as an adaptation to time via component exchange, caused by the internal kinetic and thermodynamic properties of the constituents.

It is important to note that network switching achieves a much larger change in distribution[24] (by factors of 3 to 6) than simple amplification from a statistical distribution, as described previously.[9c−e] Such large changes resulting from kinetic factors represent a very significant feature of the behavior of networks.

2.2. Kinetic Switching of CDNs of Ligand Constituents Driven by Metal Cations of Different Coordination Geometries. *2.2.1. Effects of Metal Cations on the Behavior of DCLs of Ligands.* The behavior of a DCL of ligands may be expected to be strongly influenced by the presence of metal cations in a cation specific fashion. We thus investigated whether a switching from a kinetic distribution to a thermodynamic one could also be achieved in a DCL by competition for coordination of two different metal cation effectors **M1** and **M2**, that is, switching the CDN from that favored by one metal ion to that favored by the other one on the basis of the difference in both the rate of formation of the respective ligands in the presence of the cations and relative stabilities of the two generated complexes.[25,26] The evolution of a system undergoing such a CDN switching is represented in Scheme 4. To achieve

Scheme 4. Evolution of a DCL of Four Ligand Constituents Undergoing a Time-Dependent Switching of Its Associated [2 × 2] CDN Driven by the Formation of the Complexes of Two Different Metal Cations M1 and M2

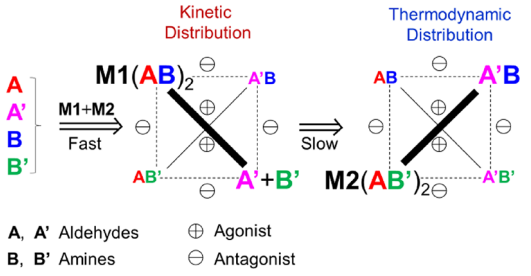

this goal requires to select components that will generate ligand constituents corresponding to the coordination geometries of different metal ions. It is known that Ag(I) forms preferentially tetracoordinated metal complexes with bidentate ligands whereas Zn(II) forms hexacoordinated octahedral complexes with tridentate ligands. Taking into account these coordination features together with the stabilities of metal complexes,[27,28] our aim was to produce kinetic switching from a tetrahedral complex to an octahedral one under the action of the two metal cation effectors, Ag(I) and Zn(II). To this end, the behavior of the **DCL**[**4**] (**A3** + **A6** + **B4** + **B5**) in the presence of both Ag(I) and Zn(II) cations was investigated.

2.2.2. Kinetic and Thermodynamic Features of Three DCLs ([4], [5], and [6]) of Four Ligand Constituents Generated from Four Components in the Presence of Metal Cations. 2.2.2.1. DCL[4]. After exploration of different component combinations, the **DCL**[**4**] based on **A3** + **A6** + **B4** + **B5** was selected to generate four constituents, comprising in particular the imine-based ligands **A3B4** and **A3B5** presenting different coordination features. The time dependence of its composition was studied in the presence of both **Ag**OTf and **Zn**$(OTf)_2$.

One may note that in the process, cation binding by a component may influence the kinetic behavior of that component. Thus, it was found in a separate experiment that Zn(II) binds to the pyridyl-hydrazine **B5** to give $[\mathbf{Zn}(\mathbf{B5})_2]^{2+}$ (see Figures S54−S56 in SI). Furthermore, one also notes that the metal cations may catalyze component exchange between the ligand constituents and thus facilitate the recombination kinetics.[29,30]

DOI: 10.1021/jacs.9b09395
J. Am. Chem. Soc. XXXX, XXX, XXX−XXX

In order to be able to identify the entities present in the rather complicated mixtures, the ^{1}H NMR spectra of all individual components and constituents were measured in the absence and in the presence of the same metal salts **Ag**OTf and **Zn**$(OTf)_2$ separately as well as together (see Figures S57−S70 in SI).

A3 + **A6** + **B4** + **B5** (10 mM, 1 equiv each), **Ag**OTf (5 mM, 0.5 equiv), and **Zn**$(OTf)_2$ (5 mM, 0.5 equiv) were mixed together in CD_3CN at room temperature and the behavior of the mixture was followed by ^{1}H NMR as a function of time (Figures 6 and S71). As shown in Figures 7 and S72, after 1 h, the silver

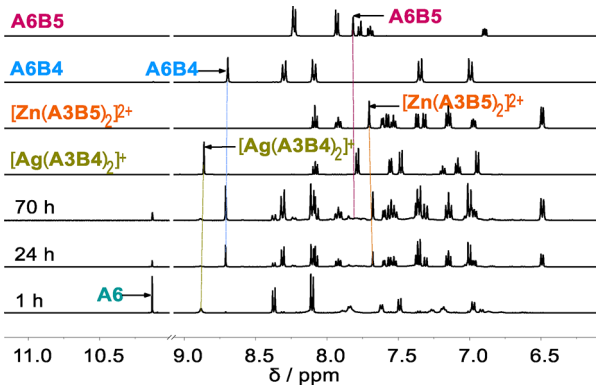

Figure 6. Evolution of ^{1}H NMR (400 MHz) spectra of the compounds generated from the **DCL**[**4**] mixture of equal amounts of **A3**, **A6**, **B4**, and **B5** (10 mM each in CD_3CN, r.t.) + 0.5 equiv. **Ag**OTf+0.5 equiv. **Zn**$(OTf)_2$ after 1 h, 24 h, and 70 h (three bottom traces). The four top traces correspond to the isolated constituents $[\mathbf{Ag}(\mathbf{A3B4})_2]^+$, $[\mathbf{Zn}(\mathbf{A3B5})_2]^{2+}$, **A6B4**, and **A6B5**. The arrows indicate the aldehyde CHO proton (9.5−10.0 ppm region) and imine CH═N proton NMR signals of the compounds.

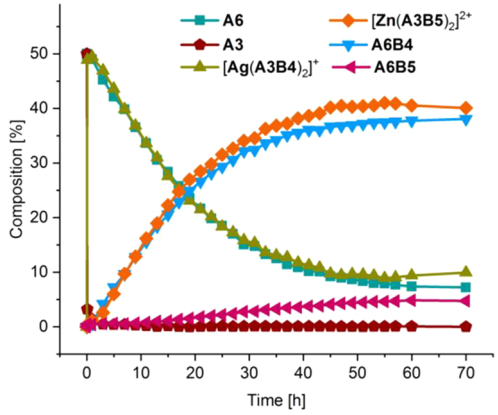

Figure 7. Kinetic plots of the evolution of a mixture of equal amounts of components **A3** + **A6** + **B4** + **B5** (10 mM each) together with 0.5 equiv. **Ag**OTf + 0.5 equiv. **Zn**$(OTf)_2$ as a function of time. The composition % data have been obtained by integration of the imine CH═N and aldehyde CHO proton signals in the 500 MHz ^{1}H NMR spectra (CD_3CN, r.t.) (see Figures S71, S72 and Table S18 in SI). For clarity, the kinetic curves are shown for only some of the compounds (see notes S21 and S22).

complex $[\mathbf{Ag}(\mathbf{A3B4})_2]^+$ of **A3B4** had fully formed together with 48% unreacted **A6** and 50% **B5** as its zinc complex. The solution was then left at r.t. for 3 days to reach equilibrium (2 days at 60 °C). The silver complex $[\mathbf{Ag}(\mathbf{A3B4})_2]^+$ strongly decreased and the formation of the zinc complex $[\mathbf{Zn}(\mathbf{A3B5})_2]^{2+}$ (see crystal structure in SI) was observed together with amplification of its agonist **A6B4**. At equilibrium, the switched library gave a distribution of 10% $[\mathbf{Ag}(\mathbf{A3B4})_2]^+$, 41% $[\mathbf{Zn}(\mathbf{A3B5})_2]^{2+}$, 38% **A6B4**, 6% **A6B5** as well as 5% free **A6**, 3% **B4** and 2% **B5** (Figures S71, S72, and Table S18). Thus, the [2 × 2] CDN associated with the **DCL**[**4**] had undergone an orthogonal kinetic switching between two metal cation complexes of different coordination geometries from the kinetic product $[\mathbf{Ag}(\mathbf{A3B4})_2]^+$ together with [**A6**+**B5**] to the thermodynamic one $[\mathbf{Zn}(\mathbf{A3B5})_2]^{2+}$ and **A6B4**. The switching process is represented in Scheme 5. In the course of this experiment one

Scheme 5. Kinetic Switching of the [2 × 2] CDN Formed by the DCL[4] Set of Components [A3 + A6 + B4 + B5] (Top) from the {$[\mathbf{Ag}(\mathbf{A3B4})_2]^+$, [A6 + B5]} State (Middle Left) To the Orthogonal State {$[\mathbf{Zn}(\mathbf{A3B5})_2]^{2+}$, A6B4} (Middle Right) (in CD_3CN at r.t.) after 1 h (Left) and after 70 h (Right)[a]

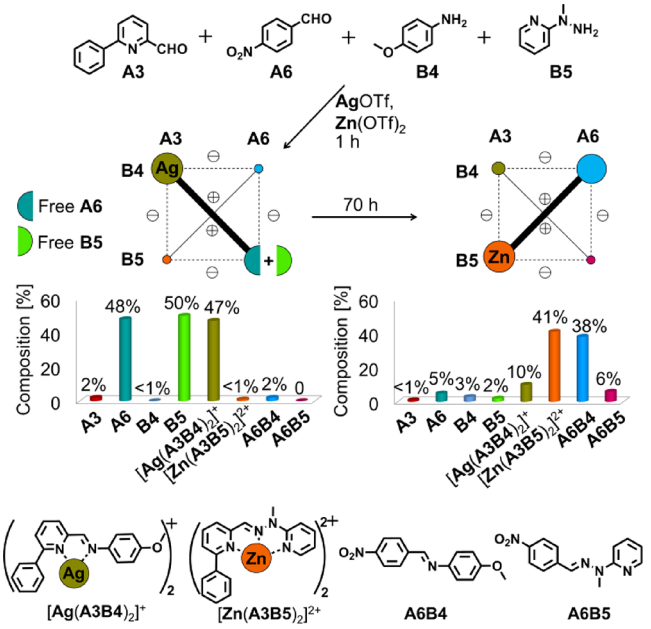

[a]The indicated composition % values of the different compounds present correspond to reaction times of 1 h (left) and 70 h (right), see also Table S18 and Figure S72 in the SI. Free anions are not indicated. Data obtained from the 500 MHz ^{1}H NMR spectra (see Figures 6 and 7).

observes that the ^{1}H NMR signals become broad after about 1 h. To test the possibility that this could be due to the interaction of ligand **A3B4** with both silver and zinc cations, an experiment was conducted where a solution of $[\mathbf{Ag}(\mathbf{A3B4})_2]^+$ was titrated with **Zn**$(OTf)_2$ (Figure S73). The ^{1}H NMR imine peak of the silver complex first became broad when 0.1 equiv. **Zn**$(OTf)_2$ was added and became broader as more zinc was added. Finally, with 1.0 equiv. **Zn**$(OTf)_2$, the spectrum was the same as that of separately prepared $[\mathbf{Zn}(\mathbf{A3B4})_2]^{2+}$, showing that initial broadening was due to interaction with the zinc cation which displaces progressively the silver cation and takes up all the **A3B4** ligand. One also notes that in the absence of metal cations no such kinetic switching is observed, indicating that the switching behavior is enforced by the metal cations.

2.2.2.2. DCL[5]. To test whether switching may also be achieved with 2-pyridinecarboxaldehyde bearing different substituents, **A3** was replaced by the methyl-bearing aldehyde **A7** and the behavior of **DCL**[**5**] generated from **A6**, **A7**, **B4**, and **B5** was studied in the presence of both **Ag**OTf and **Zn**$(OTf)_2$ (Scheme S5). From the ^{1}H NMR spectra (Figure S74), after 1 h

DOI: 10.1021/jacs.9b09395
J. Am. Chem. Soc. XXXX, XXX, XXX−XXX

the silver complex $[\mathbf{Ag}(\mathbf{A7B4})_2]^+$ (see crystal structure in SI) of **A7B4** was almost fully formed (49%) together with unreacted **A6** and **B5** due to the slow rate of hydrazone formation. After 1 day, the silver complex $[\mathbf{Ag}(\mathbf{A7B4})_2]^+$ had decreased and the zinc complex $[\mathbf{Zn}(\mathbf{A7B5})_2]^{2+}$ (see crystal structure in the SI) had appeared and then increased with simultaneous amplification of its agonist compound **A6B4**. The kinetic curves are shown in Figure S75. The equilibrium was reached after heating at 60 °C for 2 days. The final distribution of the DCL was $[\mathbf{Ag}(\mathbf{A7B4})_2]^+$ (11%), $[\mathbf{Zn}(\mathbf{A7B5})_2]^{2+}$ (39%), and **A6B4** (40%) together with 10% of free **A6** and **B5** (Table S19 and Figures S74−S76).

Similar results were obtained when **A7** was replaced by 6-bromopyridine aldehyde **A8** (see **DCL[6]** in SI Scheme S6, Figures S77−S79, and Table S20 and crystal structure for $[\mathbf{Ag}(\mathbf{A8B4})_2]^+$).

Taken together, the operation of the switching process may be attributed to the following features of the present systems:

(i) the formation of the hydrazone-based zinc complex $[\mathbf{Zn}(\mathbf{A3B5})_2]^{2+}$ is much slower than the formation of imine-based silver complex$[\mathbf{Ag}(\mathbf{A3B4})_2]^+$;

(ii) the zinc complex $[\mathbf{Zn}(\mathbf{A3B5})_2]^{2+}$ of the tridentate hydrazone **A3B5** is thermodynamically more stable than the silver complex $[\mathbf{Ag}(\mathbf{A3B4})_2]^+$ of the bidentate imine **A3B4**;

(iii) trapping of Zn(II) by binding to the pyridyl-hydrazine **B5** to give $[\mathbf{Zn}(\mathbf{B5})_2]^{2+}$ (see above and Figures S54−S56 in SI) may be expected to slow down the formation of the $[\mathbf{Zn}(\mathbf{A3B5})_2]^{2+}$ complex thus allowing the silver complex with the imine constituent $[\mathbf{Ag}(\mathbf{A3B4})_2]^+$ to form first.

The three metallo-DCLs described here present orthogonal network switching of the corresponding CDNs from one diagonal to the other diagonal of the [2 × 2] square, from a nonequilibrium state to an equilibrium state under the action of the two metal cation effectors, Ag(I) and Zn(II) as a function of time. The kinetic up-regulation amounts to a factor of at least 20 for the constituents **A6B4** and $[\mathbf{Zn}(\mathbf{A3B5})_2]^{2+}$.[24]

3. CONCLUSIONS

The present results demonstrate that the constitutional dynamic libraries (CDLs) investigated here achieve a time-dependent switching of the underlying [2 × 2] CDNs from kinetic to thermodynamic distributions of constituents by selective screening of the appropriate aldehyde and amino components (amine, hydroxylamine, hydrazine, hydrazide). Such a kinetic switching was realized in the absence (section 2.1) as well as in the presence of metal cations (section 2.2). The design of these CDLs rests on the selection of components displaying the appropriate interplay between kinetic and thermodynamic properties. It involves several determining factors.

(1) The formation rates usually decrease and the thermodynamic stabilities increase along the sequence of (aliphatic) imine, acylhydrazone, hydrazone, and oxime.[31]

(2) In view of the difference in reactivities of the aldehyde and amino components, the formation kinetics and distribution of the imine constituents of the DCL can be modulated over a large range of reaction rates and thermodynamic stabilities.

(3) In the presence of metal cations, as summarized above, the network switching results from the kinetics of complex formation, the relative stabilities of the complexes and eventual ancillary interactions between metal cations and components.

(4) Importantly, for both cases, in the absence as well as in the presence of metal cations, the switching behavior was obtained by simply mixing the components of the DCL, indicating that it resulted solely from the internal kinetic and thermodynamic properties of the system.

(5) On the basis of the above general considerations, the adaptation of the CDNs to the kinetics of C═N bond formation as well as to the relative stabilities of the constituents generated time-depended distributions resulting in a network switching.

The present work explicitly implements network switching driven by internal kinetic factors and thermodynamic properties in the self-contained CDNs. The very large constituent amplification (from 3 to 20 times or more) represents an adaptation to time, a significant step in the adaptive behavior of dynamic covalent systems. It paves the way to further exploration of time-dependent adaptive behavior in constitutional and reactional[3f] dynamic networks in constitutional dynamic chemistry. The results described also bear relationship to the behavior of out-of-equilibrium systems opening toward higher level kinetic behavior (for instance in training processes)[9d] in adaptive chemistry.

■ ASSOCIATED CONTENT

Supporting Information

The Supporting Information is available free of charge on the ACS Publications website at DOI: 10.1021/jacs.9b09395.

Notes on instrument and experimental details, synthetic procedures, and characterization of compounds, quantitative NMR spectra, kinetic traces, composition tables, crystal structures, and data (PDF)

■ AUTHOR INFORMATION

Corresponding Author

*lehn@unistra.fr

ORCID

Jean-Marie Lehn: 0000-0001-8981-4593

Notes

The authors declare no competing financial interest.

■ ACKNOWLEDGMENTS

We thank the ERC (Advanced Research Grant SUPRADAPT 290585), the USIAS, and the University of Strasbourg for financial support. M.H. gratefully acknowledges a doctoral fellowship from the China Scholarship Council. M.H. thanks Prof. Jack Harrowfield, Dr. Jean-François Ayme, Dr. Artem Osypenko, Dr. Youssef Atoini for extensive helpful discussions of the experimental results, as well as Dr. Jean-Louis Schmitt and Cyril Antheaume for discussion on NMR experiments.

■ REFERENCES

(1) (a) Mainzer, K. *Thinking in Complexity*; Springer-Verlag: Berlin/Heidelberg, 1994; pp 1−347. (b) Strogatz, S. H. Exploring Complex Networks. *Nature* **2001**, *410*, 268−276. (c) Lehn, J. M. From Supramolecular Chemistry towards Constitutional Dynamic Chemistry and Adaptive Chemistry. *Chem. Soc. Rev.* **2007**, *36*, 151−160. (d) Cohen, R.; Havlin, S. *Complex Networks*; Cambridge University Press: Cambridge, 2010; pp 1−238. (e) Nicolis, G.; Nicolis, C. *Foundations of Complex Systems*; World Scientific: Singapore, 2012; pp 1−328. (f) Cougnon, F. B. L.; Sanders, J. K. M. Evolution of Dynamic

DOI: 10.1021/jacs.9b09395
J. Am. Chem. Soc. XXXX, XXX, XXX−XXX

Combinatorial Chemistry. *Acc. Chem. Res.* **2012**, *45*, 2211−2221. (g) Lutz, J.-F.; Lehn, J.-M.; Meijer, E. W.; Matyjaszewski, K. From Precision Polymers to Complex Materials and Systems. *Nat. Rev. Mater.* **2016**, *1*, 16024. (h) Ashkenasy, G.; Hermans, T. M.; Otto, S.; Taylor, A. F. Systems Chemistry. *Chem. Soc. Rev.* **2017**, *46*, 2543−2554.

(2) (a) Lehn, J.-M.; Eliseev, A. V. Dynamic Combinatorial Chemistry. *Science* **2001**, *291*, 2331−2332. (b) Rowan, S. J.; Cantrill, S. J.; Cousins, G. R. L.; Sanders, J. K. M.; Stoddart, J. F. Dynamic Covalent Chemistry. *Angew. Chem., Int. Ed.* **2002**, *41*, 898−952. (c) Corbett, P. T.; Leclaire, J.; Vial, L.; West, K. R.; Wietor, J.-L.; Sanders, J. K. M.; Otto, S. Dynamic Combinatorial Chemistry. *Chem. Rev.* **2006**, *106*, 3652−3711. (d) Sadownik, J. W.; Ulijn, R. V. Dynamic Covalent Chemistry in Aid of Peptide Self-Assembly. *Curr. Opin. Biotechnol.* **2010**, *21*, 401−411. (e) Belowich, M. E.; Stoddart, J. F. Dynamic Imine Chemistry. *Chem. Soc. Rev.* **2012**, *41*, 2003−2024. (f) Gasparini, G.; Dal Molin, M.; Lovato, A.; Prins, J. P. Dynamic Covalent Chemistry. *Supramol. Chem. From Mol. to Nanomater.*; Gale, P. A., Steed, J. W., Eds.; John Wiley & Sons Ltd: Chichester, U.K., 2012; *41*, pp 1−29. (g) Luisier, N.; Schenk, K.; Severin, K. A Four-Component Organogel Based on Orthogonal Chemical Interactions. *Chem. Commun.* **2014**, *50*, 10233−10236. (h) Jin, Y.; Yu, C.; Denman, R. J.; Zhang, W. Recent Advances in Dynamic Covalent Chemistry. *Chem. Soc. Rev.* **2013**, *42*, 6634−6654. (i) Li, J.; Nowak, P.; Otto, S. Dynamic Combinatorial Libraries: From Exploring Molecular Recognition to Systems Chemistry. *J. Am. Chem. Soc.* **2013**, *135*, 9222−9239.

(3) (a) Constitutional Dynamic Chemistry; Barboiu, M., Ed.; *Topics in Current Chemistry*; Springer: Berlin/Heidelberg, 2012, *322*, pp 1−314. (b) Herrmann, A. Dynamic Combinatorial/Covalent Chemistry: a Tool to Read, Generate and Modulate the Bioactivity of Compounds and Compound Mixtures. *Chem. Soc. Rev.* **2014**, *43*, 1899−1933. (c) Zhang, W.; Jin, Y. *Dynamic Covalent Chemistry*; Zhang, W., Jin, Y., Eds.; John Wiley & Sons Ltd: Chichester, U.K., 2017; pp 1−464. (d) Giuseppone, N.; Lehn, J. M. Protonic and Temperature Modulation of Constituent Expression by Component Selection in a Dynamic Combinatorial Library of Imines. *Chem. - Eur. J.* **2006**, *12*, 1715−1722. (e) Hafezi, N.; Lehn, J. M. Adaptation of Dynamic Covalent Systems of Imine Constituents to Medium Change by Component Redistribution under Reversible Phase Separation. *J. Am. Chem. Soc.* **2012**, *134*, 12861−12868. (f) Armao, J. J.; Lehn, J. M. Nonlinear Kinetic Behavior in Constitutional Dynamic Reaction Networks. *J. Am. Chem. Soc.* **2016**, *138*, 16809−16814. (g) Dhers, S.; Holub, J.; Lehn, J.-M. Coevolution and Ratiometric Behaviour in Metal Cation-Driven Dynamic Covalent Systems. *Chem. Sci.* **2017**, *8*, 2125−2130. (h) Wang, S.; Yue, L.; Shpilt, Z.; Cecconello, A.; Kahn, J. S.; Lehn, J.-M.; Willner, I. Controlling the Catalytic Functions of DNAzymes within Constitutional Dynamic Networks of DNA Nanostructures. *J. Am. Chem. Soc.* **2017**, *139*, 9662−9671. (i) Yue, L.; Wang, S.; Cecconello, A.; Lehn, J. M.; Willner, I. Orthogonal Operation of Constitutional Dynamic Networks Consisting of DNA-Tweezer Machines. *ACS Nano* **2017**, *11*, 12027−12036. (j) Yue, L.; Wang, S.; Lilienthal, S.; Wulf, V.; Remacle, F.; Levine, R. D.; Willner, I. Intercommunication of DNA-Based Constitutional Dynamic Networks. *J. Am. Chem. Soc.* **2018**, *140*, 8721−8731. (k) Zhou, Z.; Yue, L.; Wang, S.; Lehn, J.-M.; Willner, I. DNA-Based Multiconstituent Dynamic Networks: Hierarchical Adaptive Control over the Composition and Cooperative Catalytic Functions of the Systems. *J. Am. Chem. Soc.* **2018**, *140*, 12077−12089. (l) Hewitt, S. H.; Wilson, A. J. Generation of Dynamic Combinatorial Libraries Using Hydrazone-Functionalized Surface Mimetics. *Eur. J. Org. Chem.* **2018**, *2018*, 1872−1879.

(4) (a) Lehn, J.-M. Dynamic Combinatorial Chemistry and Virtual Combinatorial Libraries. *Chem. - Eur. J.* **1999**, *5*, 2455−2463. (b) Brisig, B.; Sanders, J. K. M.; Otto, S. Selection and Amplification of a Catalyst from a Dynamic Combinatorial Library. *Angew. Chem., Int. Ed.* **2003**, *42*, 1270−1273. (c) Turega, S. M.; Lorenz, C.; Sadownik, J. W.; Philp, D. Target-Driven Selection in a Dynamic Nitrone Library. *Chem. Commun.* **2008**, 4076−4078. (d) Xu, S.; Giuseppone, N. Self-Duplicating Amplification in a Dynamic Combinatorial Library. *J. Am. Chem. Soc.* **2008**, *130*, 1826−1827. (e) Fujii, S.; Lehn, J.-M. Structural and Functional Evolution of a Library of Constitutional Dynamic Polymers Driven by Alkali Metal Ion Recognition. *Angew. Chem., Int. Ed.* **2009**, *48*, 7635−7638. (f) Barboiu, M.; Dumitru, F.; Legrand, Y.-M.; Petit, E.; van der Lee, A. Self-Sorting of Equilibrating Metallosupramolecular DCLs via Constitutional Crystallization. *Chem. Commun.* **2009**, 2192−2194. (g) Barboiu, M. Dynamic Interactive Systems: Dynamic Selection in Hybrid Organic−Inorganic Constitutional Networks. *Chem. Commun.* **2010**, *46*, 7466−7476. (h) Miller, B. L. Dynamic Covalent Chemistry: Catalysing Dynamic Libraries. *Nat. Chem.* **2010**, *2*, 433−434. (i) del Amo, V.; Philp, D. Integrating Replication-Based Selection Strategies in Dynamic Covalent Systems. *Chem. - Eur. J.* **2010**, *16*, 13304−13318. (j) Hunt, R. A. R.; Otto, S. Dynamic Combinatorial Libraries: New Opportunities in Systems Chemistry. *Chem. Commun.* **2011**, *47*, 847−858. (k) Rancan, M.; Tessarolo, J.; Casarin, M.; Zanonato, P. L.; Quici, S.; Armelao, L. Double Level Selection in a Constitutional Dynamic Library of Coordination Driven Supramolecular Polygons. *Inorg. Chem.* **2014**, *53*, 7276−7287.

(5) (a) Vantomme, G.; Lehn, J.-M. Reversible Adaptation to Photoinduced Shape Switching by Oligomer-Macrocycle Interconversion with Component Selection in a Three-State Constitutional Dynamic System. *Chem. - Eur. J.* **2014**, *20*, 16188−16193. (b) Vantomme, G.; Hafezi, N.; Lehn, J.-M. A Light-Induced Reversible Phase Separation and Its Coupling to a Dynamic Library of Imines. *Chem. Sci.* **2014**, *5*, 1475−1483. (c) Ji, S.; Cao, W.; Yu, Y.; Xu, H. Dynamic Diselenide Bonds: Exchange Reaction Induced by Visible Light without Catalysis. *Angew. Chem., Int. Ed.* **2014**, *53*, 6781−6785. (d) Kathan, M.; Kovaříček, P.; Jurissek, C.; Senf, A.; Dallmann, A.; Thünemann, A. F.; Hecht, S. Control of Imine Exchange Kinetics with Photoswitches to Modulate Self-Healing in Polysiloxane Networks by Light Illumination. *Angew. Chem., Int. Ed.* **2016**, *55*, 13882−13886. (e) Kassem, S.; Lee, A. T. L.; Leigh, D. A.; Markevicius, A.; Solà, J. Pick-up, Transport and Release of a Molecular Cargo Using a Small-molecule Robotic Arm. *Nat. Chem.* **2016**, *8*, 138−143. (f) Cvrtila, I.; Fanlo-Virgós, H.; Schaeffer, G.; Monreal Santiago, G.; Otto, S. Redox Control over Acyl Hydrazone Photoswitches. *J. Am. Chem. Soc.* **2017**, *139*, 12459−12465. (g) Herder, M.; Lehn, J.-M. The Photodynamic Covalent Bond: Sensitized Alkoxyamines as a Tool to Shift Reaction Networks Out-of-Equilibrium Using Light Energy. *J. Am. Chem. Soc.* **2018**, *140*, 7647−7657.

(6) Mukherjee, S.; Cash, J. J.; Sumerlin, B. S. *Responsive Dynamic Covalent Polymers*; Zhang, W., Jin, Y., Eds.; John Wiley & Sons, Ltd: Chichester, U.K., 2018; pp 321−358.

(7) Sobczak, S.; Drożdż, W.; Lampronti, G. I.; Belenguer, A. M.; Katrusiak, A.; Stefankiewicz, A. R. Dynamic Covalent Chemistry under High-Pressure: a New Route to Disulfide Metathesis. *Chem. - Eur. J.* **2018**, *24*, 8769−8773.

(8) (a) Giuseppone, N.; Fuks, G.; Lehn, J.-M. Tunable Fluorene-Based Dynamers through Constitutional Dynamic Chemistry. *Chem. - Eur. J.* **2006**, *12*, 1723−1735. (b) Giuseppone, N.; Lehn, J.-M. Electric-Field Modulation of Component Exchange in Constitutional Dynamic Liquid Crystals. *Angew. Chem., Int. Ed.* **2006**, *45*, 4619−4624. (c) Zhang, Y.; Barboiu, M. Mechanism Insight into the Constitutional Phase Change Selection of Dynameric Framework Libraries. *ACS Omega* **2018**, *3*, 329−333.

(9) (a) Giuseppone, N.; Schmitt, J. L.; Lehn, J. M. Driven Evolution of a Constitutional Dynamic Library of Molecular Helices toward the Selective Generation of [2 × 2] Gridlike Arrays under the Pressure of Metal Ion Coordination. *J. Am. Chem. Soc.* **2006**, *128*, 16748−16763. (b) Klein, J. M.; Saggiomo, V.; Reck, L.; Lüning, U.; Sanders, J. K. M. Dynamic Combinatorial Libraries for the Recognition of Heavy Metal Ions. *Org. Biomol. Chem.* **2012**, *10*, 60−66. (c) Vantomme, G.; Jiang, S.; Lehn, J.-M. Adaptation in Constitutional Dynamic Libraries and Networks, Switching between Orthogonal Metalloselection and Photoselection Processes. *J. Am. Chem. Soc.* **2014**, *136*, 9509−9518. (d) Holub, J.; Vantomme, G.; Lehn, J.-M. Training a Constitutional Dynamic Network for Effector Recognition: Storage, Recall, and Erasing of Information. *J. Am. Chem. Soc.* **2016**, *138*, 11783−11791. (e) Men, G.; Lehn, J.-M. Higher Order Constitutional Dynamic

DOI: 10.1021/jacs.9b09395
J. Am. Chem. Soc. XXXX, XXX, XXX−XXX

Networks: [2 × 3] and [3 × 3] Networks Displaying Multiple, Synergistic and Competitive Hierarchical Adaptation. *J. Am. Chem. Soc.* **2017**, *139*, 2474−2483. (f) Osypenko, A.; Dhers, S.; Lehn, J.-M. Pattern Generation and Information Transfer through a Liquid/Liquid Interface in 3D Constitutional Dynamic Networks of Imine Ligands in Response to Metal Cation Effectors. *J. Am. Chem. Soc.* **2019**, *141*, 12724−12737.

(10) (a) Tauk, L.; Schröder, A. P.; Decher, G.; Giuseppone, N. Hierarchical Functional Gradients of pH-Responsive Self-Assembled Monolayers Using Dynamic Covalent Chemistry on Surfaces. *Nat. Chem.* **2009**, *1*, 649−656. (b) Bracchi, M. E.; Fulton, D. A. Orthogonal Breaking and Forming of Dynamic Covalent Imine and Disulfide Bonds in Aqueous Solution. *Chem. Commun.* **2015**, *51*, 11052−11055. (c) Wang, Y.; Xing, P.; An, W.; Ma, M.; Yang, M.; Luan, T.; Tang, R.; Wang, B.; Hao, A. pH-Responsive Dipeptide-Based Dynamic Covalent Chemistry Systems Whose Products and Self-Assemblies Depend on the Structure of Isomeric Aromatic Dialdehydes. *Langmuir* **2018**, *34*, 13725−13734. (d) Ren, Y.; Svensson, P. H.; Ramström, O. A Multi-Controlled Enamine Configurational Switch Undergoing Dynamic Constitutional Exchange. *Angew. Chem., Int. Ed.* **2018**, *57*, 6256−6260.

(11) (a) Ramström, O.; Lehn, J.-M. Drug Discovery by Dynamic Combinatorial Libraries. *Nat. Rev. Drug Discovery* **2002**, *1*, 26−36. (b) Mondal, M.; Hirsch, A. K. H. Dynamic Combinatorial Chemistry: a Tool to Facilitate the Identification of Inhibitors for Protein Targets. *Chem. Soc. Rev.* **2015**, *44*, 2455−2488. (c) Ren, Y.; You, L. Dynamic Signaling Cascades: Reversible Covalent Reaction-Coupled Molecular Switches. *J. Am. Chem. Soc.* **2015**, *137*, 14220−14228. (d) Frei, P.; Hevey, R.; Ernst, B. Dynamic Combinatorial Chemistry: A New Methodology Comes of Age. *Chem. - Eur. J.* **2019**, *25*, 60−73. (e) Zou, H.; Hai, Y.; Ye, H.; You, L. Dynamic Covalent Switches and Communicating Networks for Tunable Multicolor Luminescent Systems and Vapor Responsive Materials. *J. Am. Chem. Soc.* **2019**, *141*, 16344.

(12) (a) Nitschke, J. R.; Lehn, J.-M. Self-Organization by Selection: Generation of a Metallosupramolecular Grid Architecture by Selection of Components in a Dynamic Library of Ligands. *Proc. Natl. Acad. Sci. U. S. A.* **2003**, *100*, 11970−11974. (b) Sreenivasachary, N.; Lehn, J.-M. Gelation-Driven Component Selection in the Generation of Constitutional Dynamic Hydrogels Based on Guanine-Quartet Formation. *Proc. Natl. Acad. Sci. U. S. A.* **2005**, *102*, 5938−5943. (c) Saur, I.; Scopelliti, R.; Severin, K. Utilization of Self-Sorting Processes to Generate Dynamic Combinatorial Libraries with New Network Topologies. *Chem. - Eur. J.* **2006**, *12*, 1058−1066. (d) Schultz, D.; Nitschke, J. R. Kinetic and Thermodynamic Selectivity in Subcomponent Substitution. *Chem. - Eur. J.* **2007**, *13*, 3660−3665. (e) Sreenivasachary, N.; Lehn, J.-M. Structural Selection in G-Quartet-Based Hydrogels and Controlled Release of Bioactive Molecules. *Chem. - Asian J.* **2008**, *3*, 134−139. (f) Sadownik, J. W.; Philp, D. A Simple Synthetic Replicator Amplifies Itself from a Dynamic Reagent Pool. *Angew. Chem., Int. Ed.* **2008**, *47*, 9965−9970. (g) Lao, L. L.; Schmitt, J.-L.; Lehn, J.-M. Evolution of a Constitutional Dynamic Library Driven by Self-Organisation of a Helically Folded Molecular Strand. *Chem. - Eur. J.* **2010**, *16*, 4903−4910. (h) Orrillo, A. G.; Furlan, R. L. E. Supramolecular Interactions between Library Members Modulate the Behavior of Dynamic Combinatorial Libraries. *J. Org. Chem.* **2010**, *75*, 211−214. (i) Ghosh, S.; Isaacs, L. *Complex Self-Sorting Systems*. Miller, B. L., Ed.; John Wiley & Sons, Inc: Hoboken, 2010; pp 118−154. (j) Simpson, M. G.; Pittelkow, M.; Watson, S. P.; Sanders, J. K. M. Dynamic combinatorial chemistry with hydrazones: cholate-based building blocks and libraries. *Org. Biomol. Chem.* **2010**, *8*, 1173−1180. (k) Ji, Q.; Lirag, R. C.; Miljanić, O. Š. Kinetically Controlled Phenomena in Dynamic Combinatorial Libraries. *Chem. Soc. Rev.* **2014**, *43*, 1873−1884. (l) Solà, J.; Lafuente, M.; Atcher, J.; Alfonso, I. Constitutional Self-Selection from Dynamic Combinatorial Libraries in Aqueous Solution through Supramolecular Interactions. *Chem. Commun.* **2014**, *50*, 4564−4566. (m) Schaufelberger, F.; Ramström, O. Kinetic Self-Sorting of Dynamic Covalent Catalysts with Systemic Feedback Regulation. *J. Am. Chem. Soc.* **2016**, *138*, 7836−7839. (n) Liang, C.; Kulchat, S.; Jiang, S.; Lehn, J.-M. Gelation-Driven Selection in Dynamic Covalent C═C/C═N Exchange. *Chem. Sci.* **2017**, *8*, 6822−6828. (o) Hsu, C. W.; Miljanić, O. Š. *Self-Sorting through Dynamic Covalent Chemistry*; Zhang, W., Jin, Y., Eds.; John Wiley & Sons Ltd: Chichester, UK, 2018; pp 253−284.

(13) Lehn, J.; Ulrich, S. Adaptation to Shape Switching by Component Selection in a Constitutional Dynamic System. *J. Am. Chem. Soc.* **2009**, *131*, 5546−5559.

(14) (a) Layer, R. W. The Chemistry of Imines. *Chem. Rev.* **1963**, *63*, 489−510. (b) *The Chemistry of Carbon-Nitrogen Double Bond*; Patai, S., Eds.; John Wiley & Sons Ltd, 1970; pp 1−794. (c) Zhou, Y.; Li, L.; Ye, H.; Zhang, L.; You, L. Quantitative Reactivity Scales for Dynamic Covalent and Systems Chemistry. *J. Am. Chem. Soc.* **2016**, *138*, 381−389.

(15) (a) Dirksen, A.; Dawson, P. E. Rapid Oxime and Hydrazone Ligations with Aromatic Aldehydes for Biomolecular Labeling. *Bioconjugate Chem.* **2008**, *19*, 2543−2548. (b) Blanden, A. R.; Mukherjee, K.; Dilek, O.; Loew, M.; Bane, S. L. 4-Aminophenylalanine as a Biocompatible Nucleophilic Catalyst for Hydrazone Ligations at Low Temperature and Neutral pH. *Bioconjugate Chem.* **2011**, *22*, 1954−1961. (c) Kool, E. T.; Park, D.-H.; Crisalli, P. Fast Hydrazone Reactants: Electronic and Acid/Base Effects Strongly Influence Rate at Biological pH. *J. Am. Chem. Soc.* **2013**, *135*, 17663−17666. (d) Crisalli, P.; Kool, E. T. Importance of Ortho Proton Donors in Catalysis of Hydrazone Formation. *Org. Lett.* **2013**, *15*, 1646−1649. (e) Tatum, L. A.; Su, X.; Aprahamian, I. Simple Hydrazone Building Blocks for Complicated Functional Materials. *Acc. Chem. Res.* **2014**, *47*, 2141−2149. (f) Su, X.; Aprahamian, I. Hydrazone-based Switches, Metallo-Assemblies and Sensors. *Chem. Soc. Rev.* **2014**, *43*, 1963−1981. (g) Pramanik, S.; Aprahamian, I. Hydrazone Switch-Based Negative Feedback Loop. *J. Am. Chem. Soc.* **2016**, *138*, 15142−15145.

(16) (a) Van Dijken, D. J.; Kovaříček, P.; Ihrig, S. P.; Hecht, S. Acylhydrazones as Widely Tunable Photoswitches. *J. Am. Chem. Soc.* **2015**, *137*, 14982−14991. (b) Gordillo Varela, M. A.; Zuluaga, F.; Chaur Valencia, M. N. Acylhydrazone-based Dynamic Combinatorial Libraries: Study of the Thermodynamic/Kinetic Evolution, Configurational and Coordination Dynamics. *Rev. Colomb. Quim.* **2016**, *45*, 39−50.

(17) (a) Jencks, W. P. Studies on the Mechanism of Oxime and Semicarbazone Formation. *J. Am. Chem. Soc.* **1959**, *81*, 475−481. (b) Polyakov, V. A.; Nelen, M. I.; Nazarpack-Kandlousy, N.; Ryabov, A. D.; Eliseev, A. V. Imine Exchange in O-aryl and O-alkyl Oximes As a Base Reaction for Aqueous Dynamic Combinatorial Libraries. A Kinetic and Thermodynamic Study. *J. Phys. Org. Chem.* **1999**, *12*, 357−363. (c) Dirksen, A.; Hackeng, T. M.; Dawson, P. E. Nucleophilic Catalysis of Oxime Ligation. *Angew. Chem., Int. Ed.* **2006**, *45*, 7581−7584. (d) Thygesen, M. B.; Munch, H.; Sauer, J.; Cló, E.; Jørgensen, M. R.; Hindsgaul, O.; Jensen, K. J. Nucleophilic Catalysis of Carbohydrate Oxime Formation by Anilines. *J. Org. Chem.* **2010**, *75*, 1752−1755. (e) Wendeler, M.; Grinberg, L.; Wang, X.; Dawson, P. E.; Baca, M. Enhanced Catalysis of Oxime-Based Bioconjugations by Substituted Anilines. *Bioconjugate Chem.* **2014**, *25*, 93−101. (f) Wang, S.; Gurav, D.; Oommen, O. P.; Varghese, O. P. Insights into the Mechanism and Catalysis of Oxime Coupling Chemistry at Physiological pH. *Chem. - Eur. J.* **2015**, *21*, 5980−5985. (g) Schmidt, P.; Stress, C.; Gillingham, D. Boronic Acids Facilitate Rapid Oxime Condensations at Neutral PH. *Chem. Sci.* **2015**, *6*, 3329−3333. (h) Agten, S. M.; Suylen, D. P. L.; Hackeng, T. M. Oxime Catalysis by Freezing. *Bioconjugate Chem.* **2016**, *27*, 42−46.

(18) (a) Dirksen, A.; Dirksen, S.; Hackeng, T. M.; Dawson, P. E. Nucleophilic Catalysis of Hydrazone Formation and Transimination: Implications for Dynamic Covalent Chemistry. *J. Am. Chem. Soc.* **2006**, *128*, 15602−15603. (b) Crisalli, P.; Kool, E. T. Water-Soluble Organocatalysts for Hydrazone and Oxime Formation. *J. Org. Chem.* **2013**, *78*, 1184−1189. (c) Rashidian, M.; Mahmoodi, M. M.; Shah, R.; Dozier, J. K.; Wagner, C. R.; Distefano, M. D. A Highly Efficient Catalyst for Oxime Ligation and Hydrazone-Oxime Exchange Suitable for Bioconjugation. *Bioconjugate Chem.* **2013**, *24*, 333−342. (d) Kool, E. T.; Crisalli, P.; Chan, K. M. Fast Alpha Nucleophiles: Structures That

DOI: 10.1021/jacs.9b09395
J. Am. Chem. Soc. XXXX, XXX, XXX−XXX

Undergo Rapid Hydrazone/Oxime Formation at Neutral pH. *Org. Lett.* **2014**, *16*, 1454−1457. (e) Kölmel, D. K.; Kool, E. T. Oximes and Hydrazones in Bioconjugation: Mechanism and Catalysis. *Chem. Rev.* **2017**, *117*, 10358−10376. (f) Larsen, D.; Kietrys, A. M.; Clark, S. A.; Park, H. S.; Ekebergh, A.; Kool, E. T. Exceptionally Rapid Oxime and Hydrazone Formation Promoted by Catalytic Amine Buffers with Low Toxicity. *Chem. Sci.* **2018**, *9*, 5252−5259. (g) Drienovská, I.; Mayer, C.; Dulson, C.; Roelfes, G. A Designer Enzyme for Hydrazone and oxime Formation Featuring an Unnatural Catalytic Aniline Residue. *Nat. Chem.* **2018**, *10*, 946−952.

(19) Kalia, J.; Raines, R. T. Hydrolytic Stability of Hydrazones and Oximes. *Angew. Chem., Int. Ed.* **2008**, *47*, 7523−7526.

(20) Kulchat, S.; Chaur, M. N.; Lehn, J.-M. Kinetic Selectivity and Thermodynamic Features of Competitive Imine Formation in Dynamic Covalent Chemistry. *Chem. - Eur. J.* **2017**, *23*, 11108−11118.

(21) The compositions of the DCLs given below have been determined by integration of characteristic ^{1}H NMR signals (−CHO, −CH═N, aromatic −H, $-CH_2$, $-CH_3$) with respect to the proton signal (at 0.06 ppm) of hexamethyldisiloxane (HMDSO) as internal standard. The sum of the % for each component in the different entities present in the DCL is equal to 50%, the maximum any constituent can reach. The error in ^{1}H NMR integration amounts to about 5% (see also SI for details).

(22) In view of the complicated behavior of competitive reactions in the present systems, a determination of the rate constants and a full kinetic analysis were not attempted. Furthermore, the goal was to demonstrate the occurrence of kinetic network switching, as is clearly shown by the crossing of the distribution curves in Figures 1, 3, 5, and 7. Tables S1, S2, S8, S14, and S18 in the SI provide quantitative data on the distributions at different time points.

(23) Men, G.; Lehn, J.-M. Multiple Adaptation of Constitutional Dynamic Networks and Information Storage in Constitutional Distributions of Acylhydrazones. *Chem. Sci.* **2019**, *10*, 90−98.

(24) In the previous studies, starting from a statistical distribution (about 25% of each of the four constituents) of the initial equilibrated state of the DCL, the maximum amplification achievable for a given constituent was at most twice that in the initial distribution, i.e., from 25% to a maximum of 50% (together with 50% of its agonist). The processes described here display much larger changes in distributions: they amount to a network switching from an initial state where one pair of diagonally linked agonistic constituents is almost absent to a final state where this same pair is strongly dominant and conversely for the other pair of constituents. For example, in **DCL**[**4**], the constituents $[\mathbf{Zn}(\mathbf{A3B5})_2]^{2+}$ and **A6B4** are amplified from 1% and 2%, respectively, in the initial kinetic distribution to 41% and 38% in the final thermodynamic distribution, a change by more than a factor of 20.

(25) Ayme, J.-F.; Lehn, J.-M. From Coordination Chemistry to Adaptive Chemistry. In *Adv. Inorg. Chem.*; van Eldik, R., Puchta, R., Eds.; Academic Press: Cambridge, MA, 2018; *71*, pp 3−78.

(26) (a) Uruska, I., Libus, W. The Relative Stability of Octahedral and Tetrahedral Complexes of Transition Metal Ions. In *Proceedings of the 8th International Conference on Coordination Chemistry*; Gutmann, V., Eds.; Springer: Vienna, 1964; pp 340−343. (b) Campbell, V. E.; de Hatten, X.; Delsuc, N.; Kauffmann, B.; Huc, I.; Nitschke, J. R. Cascading Transformations within a Dynamic Self-assembled System. *Nat. Chem.* **2010**, *2*, 684−687.

(27) Roberts, D. A.; Pilgrim, B. S.; Nitschke, J. R. Covalent Post-assembly Modification in MetalloSupramolecular Chemistry. *Chem. Soc. Rev.* **2018**, *47*, 626−644.

(28) Irving, H.; Williams, R. J. P. The Stability of Transition-Metal Complexes. *J. Chem. Soc.* **1953**, 3192−3210.

(29) Giuseppone, N.; Schmitt, J.-L.; Schwartz, E.; Lehn, J.-M. Scandium(III) Catalysis of Transimination Reactions. Independent and Constitutionally Coupled Reversible Processes. *J. Am. Chem. Soc.* **2005**, *127*, 5528−5539.

(30) Zhang, Y.; Xie, S.; Yan, M.; Ramström, O. Dynamic Covalent Chemistry of Aldehyde Enamines: Bi^{III}- and Sc^{III}-Catalysis of Amine−Enamine Exchange. *Chem. - Eur. J.* **2017**, *23*, 11908−11912.

(31) These sequences of relative rates and stabilities are only qualitative and may change depending on the structures of the reagents and other parameters such as solvent, pH, and so forth.

DOI: 10.1021/jacs.9b09395
J. Am. Chem. Soc. XXXX, XXX, XXX−XXX